Extended photoionization calculations for xenon

M. Kutzner, V. Radojević, and H. P. Kelly
Jesse W. Beams Laboratory of Physics, Department of Physics, University of Virginia, Charlottesville, Virginia 22901
(Received 20 June 1989)

Partial photoionization cross sections and angular distribution asymmetry parameters for atomic xenon have been calculated in the relativistic random-phase approximation for 26 *jj*-coupled channels over a wide range of energies (0–1 keV). The effects of relaxation on the 4*d* and 3*d* cross sections are examined by using a modification of the relativistic random-phase approximation that calculates excited-state orbitals in the potential of the relaxed ion. Results are compared with Hartree-Fock theory, with the nonrelativistic random-phase approximation, and with recent photoemission experiments.

I. INTRODUCTION

The photoionization of atomic xenon ($Z=54$) continues to be of considerable interest to both experimentalists[1–8] and theorists[9,10] alike. Much of the recent work has concentrated on photoionization in the vicinity of the giant 4*d* shape resonance which dominates the spectrum from the $4d_{5/2}$ threshold (67.50 eV) to the 4*d* Cooper minimum at approximately 160 eV. Becker *et al.*[1] and Kämmerling, Kossmann, and Schmidt[2] have recently performed photoemission measurements of the 4*d* partial cross section reaffirming the earlier experiments of Shannon, Codling, and West,[3] Adam,[4] and West *et al.*,[5] in particular their assumption on the strengths of multielectron processes. The experiments indicate that most of the photoabsorption in the 4*d* resonance region is due to direct photoionization of 4*d* electrons. However, the effects of electron correlation are also manifested by increased photoemission of 5*s* and 5*p* electrons in the same region[5] as well as by strong satellite photoemission.[1–5] A previous measurement,[6] which provided the first direct evidence that the emission of shakeoff electrons is one of the dominant decay modes of the $4d \rightarrow np$ resonances, estimated the satellite contribution to the total absorption to be as much as 50%. Presently, the experiments[1,2] show more modest satellite contributions of approximately 25%, in good agreement with the early estimates by El-Sherbini and Van der Wiel.[11] The many-body perturbation-theory (MBPT) calculations of Altun, Kutzner, and Kelly[9] which included interchannel coupling and relaxation effects are in good agreement with the experiments below the peak in the 4*d* cross section, but yield cross sections which are somewhat large at higher energies where the effects of photoionization-with-excitation channels on the 4*d* partial cross section have not been fully accounted for by the theory. Southworth *et al.*[7] have measured the 4*d* angular distribution asymmetry parameter β in the region of the giant resonance.

Other regions of the xenon spectrum have also been measured recently. Photoelectron spectroscopy has been used by Lindle *et al.*[8] to obtain partial cross sections and β parameters for the 4*d* and "4*p*" subshells above the Cooper minimum of the 4*d* cross section which occurs at 160 eV. The notation "4*p*" is used to indicate that the $4p_{1/2}$ channel interacts strongly with double excitations from the 4*d* subshell[12] including both satellite states ($4d^8nl$) and double photoionization channels ($4d^8kl$). Becker *et al.*[1,13] have recently studied partial cross sections for 5*p*, 5*s*, 4*d*, 4*p*, 4*s*, and 3*d* subshell photoionization between 40 and 1000 eV and Fahlmann *et al.*[14] have determined partial cross sections for 5*p* and 5*s* subshell photoionization at energies below the 4*d* thresholds.

The purpose of the present study is to determine whether interchannel coupling and relativistic effects within the relativistic random-phase approximation[15] (RRPA) can adequately describe the observed xenon partial cross sections over a wide energy range. We also investigate the effects of relaxation on the 4*d* and 3*d* cross sections using the relativistic random-phase approximation modified to include relaxation effects (RRPAR), a method previously applied to barium photoionization.[16]

II. METHOD OF CALCULATION

The present calculation includes 26 interacting *jj*-coupled channels satisfying the dipole approximation selection rules:

$$5p_{3/2} \rightarrow d_{5/2}, d_{3/2}, s_{1/2} ,$$
$$5p_{1/2} \rightarrow d_{3/2}, s_{1/2} ,$$
$$5s_{1/2} \rightarrow p_{3/2}, p_{1/2} ,$$
$$4d_{5/2} \rightarrow f_{7/2}, f_{5/2}, p_{3/2} ,$$
$$4d_{3/2} \rightarrow f_{5/2}, p_{3/2}, p_{1/2} ,$$
$$4p_{3/2} \rightarrow d_{5/2}, d_{3/2}, s_{1/2} ,$$
$$4p_{1/2} \rightarrow d_{3/2}, s_{1/2} ,$$
$$4s_{1/2} \rightarrow p_{3/2}, p_{1/2} ,$$
$$3d_{5/2} \rightarrow f_{7/2}, f_{5/2}, p_{3/2} ,$$
$$3d_{3/2} \rightarrow f_{5/2}, p_{3/2}, p_{1/2} .$$

Detailed RRPA studies of the xenon photoionization spectrum including cross sections, angular distributions, spin polarization parameters, and branching ratios have been given before.[10] In this study the calculations are extended to higher energies, include more coupled channels

than previous work, and also include relaxation effects.

Relaxation of the 4*d* hole is known to have a strong influence on the shape of the 4*d* cross section for xenon.[9,17] As the photoelectron is leaving the vicinity of the ion, the ionic core readjusts to the presence of the 4*d* hole and may also be polarized by the outgoing electron. We have approximated such effects in RRPA-type calculations by computing excited-state orbitals in the V^{N-1} potential of a relaxed ionic core.[16] Overlap integrals between orbitals of the ground state and orbitals of the relaxed ion multiply the dipole matrix elements in these calculations and lead to approximately an 11% reduction in the 4*d* cross section; in the case of barium, the reduction of the 4*d* cross section due to overlap integrals was about 20%.[16]

Strict RRPA calculations utilize the absolute values of the Dirac-Hartree-Fock (DHF) eigenvalues (obtained, for example, from the Oxford multiconfiguration Dirac-Fock code of Grant *et al.*[18]) for the photoionization thresholds. However, the RRPA-type calculations which include relaxation effects were performed using the difference in the total relativistic self-consistent energies of the neutral atom and the ion (ΔSCF energies) for the photoionization thresholds. Table I contains DHF, ΔSCF, and experimental threshold energies obtained using photoelectron spectroscopic methods[19] for all of the channels incorporated in the present calculations Note that, with the exception of the valence threshold, the ΔSCF thresholds agree better with experiment than do the DHF thresholds. For deep inner shells with many electrons such as 3*d*, the ΔSCF energies are very good.

The hole state of the relaxed ion may be placed either in the $d_{5/2}$ or the $d_{3/2}$ subshell and the choice about where the hole should be placed is somewhat arbitrary. However, since the $d_{5/2}$ has a lower ionization energy and also represents the largest *d* subshell, we have chosen to place the hole in the $d_{5/2}$ subshell. We have found the results to depend very weakly on which subshell is chosen. Details concerning the inclusion of relaxation effects in RRPAR calculations are discussed elsewhere[16] in the context of barium.

TABLE I. Photoionization threshold in eV for subshells of xenon included in the present calculations.

Subshell	DHF[a]	ΔE_{HCF}[b]	Expt.[c]
$5p_{3/2}$	11.968	11.227	12.130
$5p_{1/2}$	13.403	12.560	13.437
$5s_{1/2}$	27.488	26.472	23.40
$4d_{5/2}$	71.670	66.453	67.50
$4d_{3/2}$	73.780	68.470	69.48
$4p_{3/2}$	162.80	156.92	145.51
$4p_{1/2}$	175.58	169.44	
$4s_{1/2}$	229.40	223.02	213.32
$3d_{5/2}$	694.90	676.70	676.70
$3d_{3/2}$	708.14	689.68	689.35

[a]Absolute value of single-particle eigenvalue from Dirac-Hartree-Fock (DHF) calculations.
[b]Difference of self-consistent DHF calculations for ground state and ionic state.
[c]Reference 19.

III. RRPA RESULTS

The RRPA calculations of the photoionization cross sections of Xe from 0 to 300 eV are shown in Fig. 1 along with the experimental partial cross sections.[1,19,14] Since intensity variation among the different partial cross sections is so large, the spectra are plotted on a semilogarithmic scale. The measured data points are for Fahlman *et al.*[14] for lower energies, Becker *et al.*[1] for intermediate energies, and Lindle *et al.*[8] in the vicinity of the Cooper minimum of the 4*d* partial cross section. The Hartree-Fock method neglects relativistic effects and interchannel coupling. Thus it is instructive to compare the two theoretical predictions.

Interchannel coupling between the 5*p*, 5*s*, and 4*d* channels has radically altered the shape of the 5*s* and 5*p* cross sections relative to the single-particle results. The action of the 5*p* channels on the 5*s* cross section causes the 5*s* cross section to be higher at threshold than the HF result and to decrease to a minimum at approximately 35 eV. The effect of the 4*d* channels is to cause both the 5*p* and 5*s* cross sections to have maxima which nearly coincide with the 4*d* maximum and then decrease to minima near the Cooper minimum of the 4*d* channels. The peak values of the 4*d* and 5*s* cross sections in the RRPA are somewhat larger than experiment. Altun, Kutzner, and Kelly[9] have demonstrated that the inclusion of relaxation effects improves the 4*d* calculation in the vicinity of the peak. Amusia[20] has pointed out that in the nonrelativistic random-phase approximation with exchange (RPAE), the 5*s* cross section is larger than experiment at its maximum because the RPAE neglects the interaction between 5*s* single-vacancy states and multiply excited states, which reduces the 5*s* single-vacancy partial cross section. The spectroscopic factor, defined as the ratio of the single-excitation channel cross section to the sum of

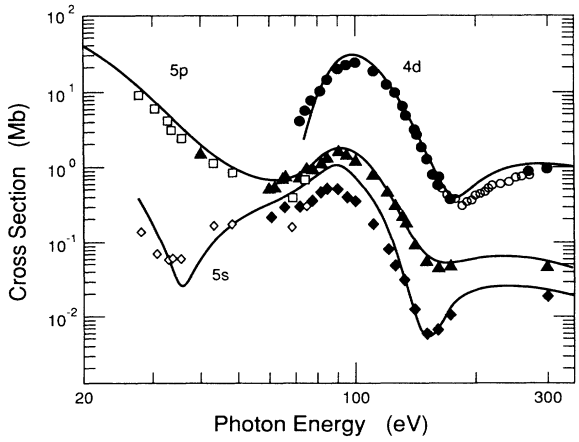

FIG. 1. Partial photoionization cross sections of xenon. RRPA represented by solid line. Measured data are from the following authors: 5*p* (□) and 5*s* (◇) by Fahlmann *et al.*, Ref. 14; 5*p* (▲), 5*s* (◆), and 4*d* (●) by Becker *et al.*, Ref. 1; and 4*d* (○) by Lindle *et al.*, Ref. 8.

the single-excitation channel and multiply excited channel cross sections, is introduced to describe this interaction.[20] By taking the ratio between the experimental[1] and the RRPA 5*s* cross sections at the peak near 100 eV, the 5*s* spectroscopic factor for xenon is approximated semiempirically to be 0.50. This value for the spectroscopic factor lies between the experimental results derived from inelastic electron scattering[21] $(e,2e)$ and photoelectron spectroscopy[22] which yield values of 0.34 and 0.6, respectively. However, we regard the photoelectron spectroscopic method to be the more fundamental method for the measurement of spectroscopic factors.

In Fig. 2 we plot the theoretical and experimental photoionization cross sections for photon energies ranging from 200 to 1 keV. Just below the 3*d* edges (about 700 eV), autoionizing resonances dominate the photoionization and were not treated in the present calculations. For photon energies above the 4*d* Cooper minimum (160 eV), there is very little difference between the single-particle model and the RRPA results. The effects of interchannel coupling appear to be reduced except very near the $3d_{5/2}$ and $3d_{3/2}$ thresholds (694.90 and 708.14 eV, respectively; see Table I). This reduction in the strength of coupling between channels for energies well above the thresholds is readily understood by noting that at higher photoelectron kinetic energies there is little time for interactions between the photoelectron and other electrons of the atom to occur.

Two different experimental results are reported for the 4*d* and 4*p* cross sections;[1] main-line cross sections and main-line plus associated double-excitation cross sections are reported. Agreement between RRPA 4*d*, 5*p*, and 5*s* cross sections and the corresponding experimental data is quite good. However, the RRPA does not agree with the measured 4*p* or 4*s* cross sections. The minimum of the measured 4*s* cross section at approximately 350 eV followed by an increase is not reproduced by the RRPA. The calculated 4*p* cross section is too large when compared with the main-line 4*p* measurement and too small above 400 eV when compared with the main-line plus satellite 4*p* measurement. The unusual behavior in these partial cross sections must result from correlation phenomena not included by the RRPA, e.g., couplings with satellite channels of the 4*d* cross section. Effects of interchannel coupling again become manifest near the 3*d* photoionization edge at approximately 700 eV where the strong 3*d* photoionization channels cause deviations of the RRPA results from the single-particle calculations in weaker channels. (The inclusion of relaxation effects in the 3*d* channel calculations reduces the peaking of the 3*d* channel cross sections as well as the cross sections of weaker channels). The 3*d* cross section is discussed later.

Figure 3 shows the behavior of the RRPA angular distribution asymmetry parameters β for the 5*p*, 5*s*, 4*d*, 4*p*, and 4*s* subshells from the valence threshold to 300 eV. The available experimental data from several sources[23–26] are plotted for comparison. The overall agreement between theory and experiment is quite good except for the 5*s* β parameter where the theoretical results dip too low compared with experiment at the Cooper minimum of the 5*s* cross section (approximately 35 eV). It is believed that, just as the 5*s* cross section is strongly influenced by interactions with doubly excited channels, the 5*s*, β parameter is also modified by such interactions in the vicinity of the Cooper minimum. Another dip in the 5*s* cross section is predicted at approximately 150 eV where the Cooper minimum in the strong 4*d* channels causes the 5*s* cross section to go through another minimum. The 4*p* β parameter is also very strongly influenced by the 4*d* channel, assuming a similar shape to the 4*d* β parameter from the 4*p* threshold to the 3*d* threshold.

Angular distribution asymmetry parameters are plotted for high energies in Fig. 4. The experimental data in

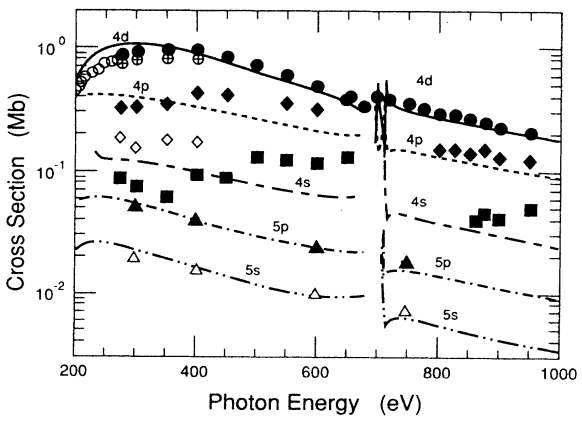

FIG. 2. Partial photoionization cross sections of xenon for energies beginning near the Cooper minimum of the 4*d* cross section. RRPA represented by the various lines 4*d* (——), 4*p* (— — —), 4*s* (— — —), 5*p* (— · — · —), and 5*s* (— · · · —). Measurements are 5*p* (▲), 5*s* (△), 4*d* (⊕), 4*p* (◇), 4*s* (■) by Becker *et al.*, Ref. 1; and 4*d* (○) by Lindel *et al.*, Ref. 8 Data for 4*d* plus associated double excitation (●) and 4*p* plus double excitation (◆) are also from Ref. 1.

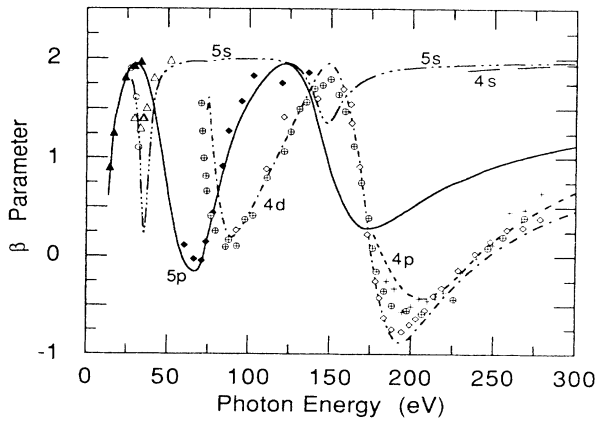

FIG. 3. Angular distribution asymmetry parameters for the photoabsorption of xenon. RRPA calculations are given by the various lined 5*p* (——), 5*s* (— · · · —), 4*d* (— · — · —), 4*p* (— — —), and 4*s* (— —). Measurements are as follows: 5*p* (▲), Ref. 23; 5*p* (◆), Ref. 24; 5*s* (○), Ref. 25; 5*s* (△), Ref. 26; 4*d* (⊕), Ref. 7; 4*d* (◇) and 4*p* (+), Ref. 8.

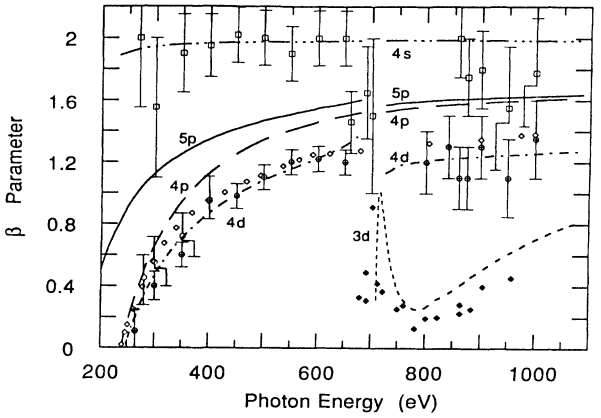

FIG. 4. Angular distribution asymmetry parameters for the photoabsorption of xenon above the Cooper minimum of the 4*d* cross section. RRPA calculations are given by the various lines 5*p* (——), 4*d* (—·—·—·), 4*p* (— — —), 4*s* (— · · · —), and 3*d* (— — —). Measured 4*d* (◇) and $3d_{5/2}$ (◆) are from Ref. 13. The open circles represent pure separated "4*p*" contributions, whereas (⊕) represent β values for sum of the "4*p*" peaks and the subsequent "continuum between "4*p*" and 4*s* from Ref. 1. Open squares represent the 4*s* β parameter from Ref. 1. The 5*s* β parameter is not plotted because it does not deviate significantly from the value of 2.0 in this energy region.

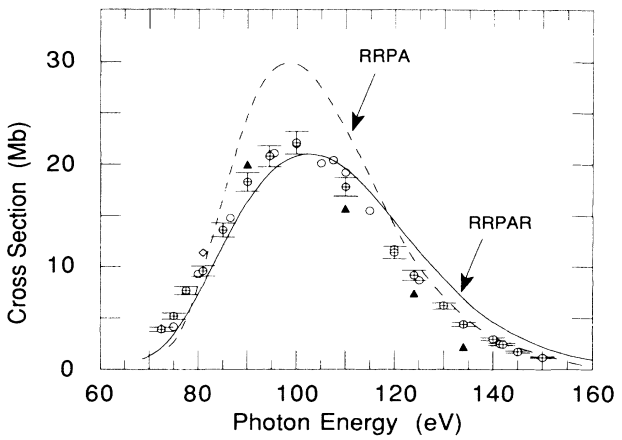

FIG. 5. Xenon partial 4*d* photoionization cross section. Curve labeled RRPA is geometric mean of unrelaxed relativistic random-phase approximation length and velocity calculations. RRPAR is the length form of cross-section calculation including relaxation effects and overlap integrals. Measured data are (⊕), Ref. 1; (○), Ref. 2; (▲), Ref. 3; and (◇), Ref. 4.

this region have been collected recently by Becker *et al.*[13] The 4*d* β parameter is in quite good agreement with experiment. The 4*p* β parameter obtained from the RRPA is somewhat larger than the measured parameter; however, we note that the 4*p* data is a sum of contributions from the 4*p* main-line channel and contributions from a "continuum' leaving the ion in a state with energy somewhere between "4*p*" and 4*s*.[1] The calculation shows very little deviation of the 4*s* β parameter from the value of 2.0 predicted by *LS* coupling, agreeing with experiment within the stated error except near the 3*d* thresholds where resonances may cause the large drop in the measured β. The RRPA 3*d* β parameter is in qualitative agreement with experiment[13] but is somewhat larger at most energie. The 5*p* and 5*s* β parameters have not been measured at these energies to our knowledge.

IV. RESULTS INCLUDING RELAXATION

Relaxation, polarization, and photoionization with excitation are important effects in photoionization which are not included in the strict RPAE or RRPA theories. Amusia *et al.*,[27] however, demonstrated that the RPAE theory could be modified to include relaxation effects. The excited orbitals are calculated in the V^{N-1} potential of a relaxed ion rather than in a frozen-core Hartree-Fock or Dirac-Hartree-Fock potential. By substituting orbitals obtained in this manner into the RPAE (Ref. 27) or RRPA (Ref. 15) equations, the effects of relaxation may be taken into account. Photoionization with excitation and double photoionization are approximately accounted for by including overlap integrals between orbitals of the initial and final states.[9]

Figure 5 shows the results of 26 channel RRPA and RRPAR calculations for the 4*d* subshell cross section. Length and velocity results are practically identical for the RRPA calculation, as they should be, and are plotted as a single line. Overlap integral factors have been included in the RRPAR calculations, reducing the partial cross section by approximately 11%. The length and velocity results agree to within approximately 5% for the RRPAR calculation, the velocity cross section being always smaller in magnitude. We have plotted the length calculation. The recent photoemission measurements by Becker *et al.*[1] and Kämmerling, Kossmann, and Schmidt[2] are plotted as well as the older data by Shannon, Codling, and West[3] and Adam.[4] Agreement between the RRPAR result and the experiments is quite good for photon energies up to the peak in the cross section. However, for energies above approximately 120 eV, the unrelaxed result is in better agreement with the experiments. This is consistent with the model used for relaxation. At low photoelectron energies, relaxation of the core occurs before the photoelectron escapes the ionic potential so that the RRPAR calculation which includes relaxation is expected to be a good approximation. For higher photoelectron energies, the photoelectron has escaped the potential before the ion has time to relax. Thus, at high energies the RRPA without relaxation is the better approximation.

The 3*d* cross section of xenon has also been shown to be sensitive to the effects of relaxation.[28] In Fig. 6 we present RRPA and RRPAR calculations of the 3*d* partial cross section in the near threshold region. Recent time-of-flight measurements by Becker *et al.*[13] are also shown in the figure. The RRPA cross section was computed using the DHF eigenvalue energies for $3d_{5/2}$ and $3d_{3/2}$ and the RRPAR calculation used ΔSCF energies (see Table I). The unrelaxed results (RRPA) has two very narrow peaks which represent separate peaks in the partial cross

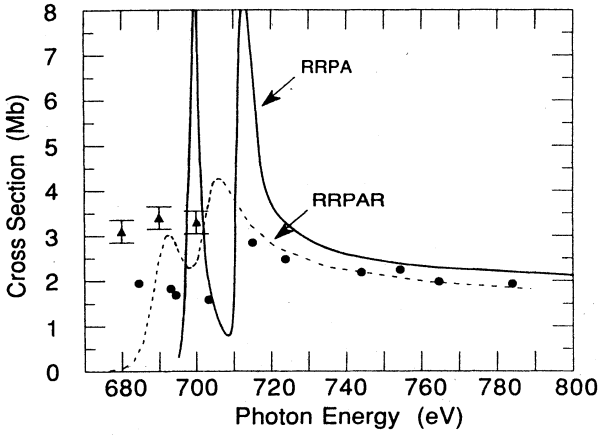

FIG. 6. Xenon partial $3d$ photoionization cross section. (——), RRPA calculation (not including relaxation). — — —, RRPAR calculation including relaxation effects and overlap integrals. (●), measured sum of $3d_{5/2}$ and $3d_{3/2}$ partial cross sections, Ref. 13. Solid triangles represent the same partial cross section measured by the corresponding MNN Auger intensity, Ref. 1.

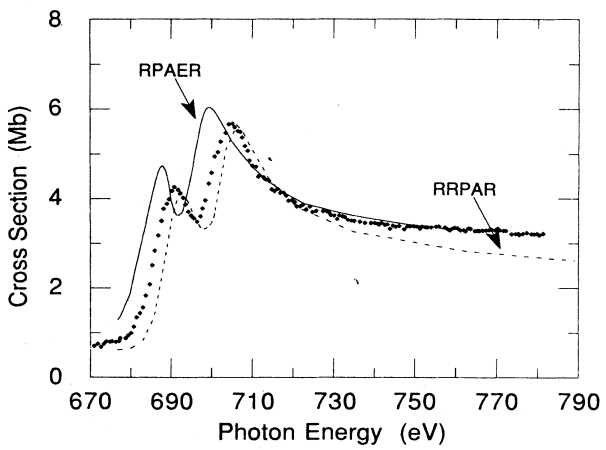

FIG. 7. Xenon total absorption cross section in the region of $3d_{5/2}$ and $3d_{3/2}$ thresholds. — — —, present RRPAR calculation, overlap integrals are not included in the RRPAR calculation of the total cross section. ——, RPAER, Ref. 28 ◆, measurements of the total absorption, Ref. 29.

sections for removing $3d_{5/2}$ and $3d_{3/2}$ electrons. The peaks are considerably higher and narrower than the peaks seen in the measured cross section.[13] The relaxed calculation (RRPAR) again shows a peak just above each threshold, but they are less abrupt and in closer agreement with experiment. Overlap integrals were included in the RRPAR calculation and cause a 16% reduction in the partial $3d$ photoionization cross section.

The RRPAR results for the total cross section in the vicinity of the $3d$ threshold are shown in Fig. 7 along with random-phase approximation with exchange including relaxation effect (RPAER) results by Amusia[28] and with the measured total absorption cross section.[29] The RRPAR calculation for the total cross section omits overlap integrals. The calculation by Amusia[28] is a nonrelativistic random-phase approximation with exchange type of calculation and includes relaxation by using excited orbitals obtained in a relaxed potential and overlap integrals evidently are not included. The RPAER result[28] was originally plotted as a function of kinetic energy of the photoelectron and has been placed on the photon energy scale by equating zero kinetic energy with our $3d_{5/2}$ ΔE_{SCF} threshold. Account is taken of the spin-orbit splitting of the thresholds of the $3d_{5/2}$ and $3d_{3/2}$ shells in the RPAER calculation[28] by assuming that, at the same energy of the removed electron, the ratio of the $3d_{5/2}$ and $3d_{3/2}$ cross sections of ionization is 1.5. The RRPAR results are in agreement with total absorption measurements[29] near threshold but are somewhat low at energies above 730 eV. This could be a reflection of the inadequacy of the relaxation model at higher energies as well as the neglect of double-photoionization and photoionization-with-excitation channels. The RPAER curve[28] appears to be in good agreement with experiment over the entire energy range. However, an earlier RPAER result presented by Amusia and Ivanov[30] is approximately 1.5 Mb lower overall and shows a peak in the $3d_{5/2}$ cross section of only 2.5 Mb; no discussion is given in the later reference[28] as to how the two RPAER calculations differ. It is not entirely clear what causes the differences between the relativistic and nonrelativistic results. The differences between the RRPAR and RPAER cross sections are due to two possible causes: (a) the RRPAR calculation includes more coupled channels than the RPAER calculation and (b) relativistic effects may play som role here. It should be noted that the RRPAR calculation of total absorption sums contributions from all singly-excited channels and does not include the reduction of the $3d$ channel due due to overlap integrals; overlap integrals were included in the calculation of the $3d$ partial cross section and approximately eliminate effects of multiple excitation resulting from shakeup processes.[31]

V. CONCLUDING REMARKS

The following conclusions may be drawn from the theoretical results presented above. First, although the RRPA results are in reasonable agreement with experimental measurements over large regions of the spectrum, there are notable exceptions where double-electron processes need to be included, namely, the $5s$ cross section in the region of the $5p$ Cooper minimum, the $4p$ cross section, and the $4s$ cross section and β parameter from threshold to the $3d$ edge where theory and experiment are in very poor agreement. It is unclear what is lacking in the RRPA treatment of these partial cross sections. Secondly, the inclusion of relaxation effects in an RRPA calculation yield results for the $4d$ partial photoionization cross section which agree quite well with experiment for energies up to and including the cross section peak. Also, the $3d$ photoionization cross section is strongly influenced by relaxation near the $3d$ threshold. The inclusion of overlap integrals which approximately account for the transfer of oscillator strength from the main-line $3d$ and $4d$ channels to doubly excited channels is essential

for a calculation of partial $3d$ and $4d$ photoionization cross sections.

ACKNOWLEDGMENTS

We wish to thank Dr. Walter Johnson for the use of the RRPA code. We also wish to thank Dr. Uwe Becker and Dr. Volker Schmidt for making their recently acquired data available to us. We thank the Academic Computing Center of The University of Virginia for a generous computing grant. Support for this work has been provided by the National Science Foundation.

[1]U. Becker, D. Szostak, H. G. Kerkhoff, M. Kupsch, B. Langer, R. Wehlitz, A. Yagishita, and T. Hayaishi, Phys. Rev. A **39**, 3902 (1989).

[2]B. Kämmerling, H. Kossmann, and V. Schmidt (unpublished).

[3]S. P. Shannon, K. Codling, and J. B. West, J. Phys. B **10**, 825 (1977).

[4]M. Y. Adam, Ph.D. thesis, Uniersité de Paris–Sud, 1978.

[5]J. B. West, P. R. Woodruff, K. Codling and R. G. Houlgate, J. Phys. B **9**, 407 (1976).

[6]U. Becker, T. Prescher, E. Schmidt, B. Sonntag, and H. E. Wetzel, Phys. Rev. A **33**, 3891 (1986).

[7]S. Southworth, U. Becker, C. M. Truesdale, Ph. H. Kobrin, D. W. Lindle, S. Owaki, and D. A Shirley, Phys. Rev. A **28**, 261 (1983).

[8]D. W. Lindle, T. A. Ferret, P. A. Heimann, and D. A. Shirley, Phys. Rev. A **37**, 3808 (1988).

[9]Z. Altun, M. Kutzner, and H. P. Kelly, Phys. Rev. A **37**, 4671 (1988).

[10]W. R. Johnson and K. T. Cheng, Phys. Rev. A **20**, 978 (1979); K.-N. Huang, W. R. Johnson, and K. T. Cheng, Phys. Rev. Lett. **43**, 1658 (1979); K.-N. Huang, W. R. Johnson, and K. T. Cheng, Phys. Lett. **77A**, 234 (1980); K.-N. Huang, W. R. Johnson, and K. T. Cheng, At. Data Nucl. Data Tables **26**, 33 (1981); K. T. Cheng and W. R. Johnson, Phys. Rev. A **28**, 2820 (1983).

[11]Th. M. El-Sherbini and M. J. Van der Wiel, Physica **62**, 110 (1972).

[12]G. Wendin and M. Ohno, Phys. Scr. **14**, 148 (1976).

[13]U. Becker, H. G. Kerkhoff, M. Kupsch, B. Langer, D. Szostak, and R. Wehlitz, J. Phys. (Paris) **48**, C9-497 (1987).

[14]A. Fahlmann, M.O. Krause, M. A. Carlson, and A. Svensson, Phys. Rev. A **30**, 812 (1984).

[15]W. R. Johnson and C. D. Lin, Phys. Rev. A **20**, 964 (1979).

[16]V. Radojević, M. Kutzner, and H. P. Kelly, Phys. Rev. A **40**, 727 (1989).

[17]M. Ya. Amusia, V. K. Ivanov, and L. V. Chernysheva, Phys. Lett. **59**, 191 (1976).

[18]I. P. Grant, B. J. McKenzie, P. H. Norrington, D. F. Mayers, and N. C. Pyper, Comput. Phys. Commun. **21**, 207 (1980).

[19]S. Svensson, N. Martensson, E. Basilier, P. A. Malmquist, U. Gelius, and G. Siegbahm, Phys. Scr. **14**, 141 (1976); K. Seigbahn, C. Nordling, G. Johansson, J. Hedman, P. F. Heden, K. Hamrin, U. Gelius. T. Bergmark, L.O. Werme, R. Manne and Y. Baer, *ESCA Applied to Free Molecules* (North-Holland, Amsterdam 1969).

[20]M. Ya. Amusia, Comments At. Mol. Phys. **16**, 143 (1985).

[21]E. Weigold and I. E. McCarthy, Adv. at Mol. Phys. **14**, 127 (1978).

[22]J. E. Hansen, Comments At. Mol. Phys. **12**, 197 (1979).

[23]M. J. Lynch, K. Codling, and A. B. Gardner, Phys. Lett. **59A**, 213 (1973).

[24]L. Torop, J. Morton, and J. B. West, J. Phys. B **9**, 2035 (1976).

[25]M. G. White, S. H. Southworth, P. Kobrin, E. D. Poliakoff, R. A. Rosenberg, and D. A. Shirley, Phys. Rev. Lett. **43**, 1661 (1979).

[26]H. Derenbach and V. Schmidt, J. Phys. B **16**, L337 (1983).

[27]M. Ya. Amusia, V. K. Ivanova, S. A. Sheinerman, S. I. Sheftel, and A. F. Ioffe, Zh. Eksp. Teor. Fiz. **78**, 910 (1980) [Sov. Phys.—JETP **51**, 458 (1980)].

[28]M. Ya. Amusia, in *Advances in Atomic and Molecular Physics*, edited by D. Bates and B. Bederson (Academic, New York, 1981), Vol. 170, p. 2.

[29]R. D. Deslattes, Phys. Rev. Lett. **20**, 483 (1968).

[30]M. Ya. Amusia and V. K. Ivanov, Phys. Lett. **65A**, 217 (1978).

[31]T. Åberg, Phys. Rev. **156**, 35 (1967).